ISSN 1674-1056
http://cpb.iphy.ac.cn
http://iopscience.iop.org/cpb
中国物理 B
Chinese Physics
中国物理 Chinese Physics B

Effect of residual Doppler averaging on the probe absorption in cascade type system: A comparative study

Suman Mondal, Arindam Ghosh, Khairul Islam, Dipankar Bhattacharyya, Amitava Bandyopadhyay

Citation: Chin. Phys. B . 2018, 27(9): 094204. **doi:** 10.1088/1674-1056/27/9/094204

Journal homepage: http://cpb.iphy.ac.cn; http://iopscience.iop.org/cpb

What follows is a list of articles you may be interested in

Coherently induced grating in refractive index enhanced medium

Zhuan-Zhuan Liu(刘撰撰), Yu-Yuan Chen(陈煜远), Jia-Yu Yuan(原佳宇), Ren-Gang Wan(万仁刚)

Chin. Phys. B . 2017, 26(12): 124209. **doi:** 10.1088/1674-1056/26/12/124209

High quality electromagnetically induced transparency spectroscopy of ^{87}Rb in a buffer gas cell with a magnetic field

Hong Cheng(成红), Han-Mu Wang(王汉睦), Shan-Shan Zhang(张珊珊), Pei-Pei Xin(辛培培), Jun Luo(罗军), Hong-Ping Liu(刘红平)

Chin. Phys. B . 2017, 26(7): 074204. **doi:** 10.1088/1674-1056/26/7/074204

Controllable double electromagnetically induced transparency in a closed four-level-loop cavity–atom system

Miao-Di Guo(郭苗迪), Xue-Mei Su(苏雪梅)

Chin. Phys. B . 2017, 26(7): 074207. **doi:** 10.1088/1674-1056/26/7/074207

Electromagnetically induced grating in a thermal N-type four-level atomic system

Ya-Bin Dong(董雅宾), Jun-Yan Li(李俊燕), Zhi-Ying Zhou(周志英)

Chin. Phys. B . 2017, 26(1): 014202. **doi:** 10.1088/1674-1056/26/1/014202

Theoretical simulation of ^{87}Rb absorption spectrum in a thermal cell

Hong Cheng(成红), Shan-Shan Zhang(张珊珊), Pei-Pei Xin(辛培培), Yuan Cheng(程元), Hong-Ping Liu(刘红平)

Chin. Phys. B . 2016, 25(11): 114203. **doi:** 10.1088/1674-1056/25/11/114203

Effect of residual Doppler averaging on the probe absorption in cascade type system: A comparative study*

Suman Mondal[1,†], Arindam Ghosh[1,‡], Khairul Islam[1], Dipankar Bhattacharyya[2], and Amitava Bandyopadhyay[1,§]

[1] *Department of Physics, Visva-Bharati, Santiniketan, PIN* 731235, *West Bengal, India*
[2] *Department of Physics, Santipur College, Santipur, PIN* 741404, *Nadia, West Bengal, India*

(Received 6 April 2018; revised manuscript received 11 June 2018; published online 28 August 2018)

Effect of residual Doppler averaging on the probe absorption in an alkali vapor medium in the presence of a coherent pump beam is studied analytically for the Ξ type system. A coherent probe field is assumed to connect the ground level with the intermediate level whereas a coherent control beam is supposed to act between the intermediate energy level and the uppermost level. Optical Bloch equations (OBE) for a three-level Ξ type system and a four-level Ξ type system are derived by using density matrix formalism. These equations are solved by an analytic method to determine the probe response, which not only depends on the wavelength difference between the control (pump) field and the probe field but shows substantially different features depending on whether the wavelength of the control field is greater than that of the probe field or the reverse. The effect of temperature on probe response is also shown. Enhancement in probe absorption and additional features are noticed under a strong probe limit at room temperature. The four-level Ξ type system has two ground levels and this leads to substantial modification in the simulated probe absorption as compared to the three-level system.

Keywords: cascade type system, density matrix method, residual Doppler averaging, electromagnetically induced transparency (EIT)

PACS: 42.50.Gy, 32.10.Fn **DOI:** 10.1088/1674-1056/27/9/094204

1. Introduction

Probe field propagation through alkali atomic vapor in the presence of a coherent control field is a topic that has been thoroughly investigated under different level schemes starting from the basic three-level Λ, Vee, and Ξ[1–3] to different multi-level systems. This has led to the prediction of electromagnetically induced transparency (EIT)[4] and its subsequent observation.[5] In multi-level systems, the probe response is often studied in the presence of more than one additional coherent fields. Y type,[6,7] inverted-Y type,[8–10] M type,[11,12] and N type[13,14] systems are prime examples of such level schemes. The applications of EIT include slowing down of probe laser beam in atomic vapor kept at room temperature,[15] stopping and storage of light,[16,17] increased higher order nonlinearity,[18,19] etc. The EIT experiment is usually done with a weak probe field and strong control field,[20] but Pandey *et al.* has observed splitting of EIT in room temperature Rb vapor by using a probe field with greater intensity compared to a pump field[21] and then termed this as the strong probe condition. They have used a Ξ type system and showed the influence of residual Doppler averaging in splitting of EIT. Salomaa *et al.*[22] first studied the effect of residual Doppler averaging in two-photon spectroscopy when the phenomenon of EIT was unknown. In the literature, many reports can be found on narrowing of the EIT line width due to Doppler averaging in measurements performed by using an alkali vapor cell at room temperature.[23,24] However, under the two-photon resonance condition, the choice of specimen as well as wavelengths of the applied fields play important roles. Shepherd *et al.*[25] showed the effect of wavelength mismatch on the probe absorption profile for a three-level Ξ type system by using theoretical as well as experimental studies. They pointed out the role played by electromagnetically induced transparency as well as Autler–Town splitting[26] due to each velocity group of atoms within the vapor in causing transparency in the probe absorption profile. Sandhya *et al.*[27] presented a theoretical study on the atomic coherence effect on a four-level system but by using three radiation fields instead of the usual two-field configuration employed in a simple Ξ type system. By using a radio-frequency field to couple two closely spaced upper levels, they showed the occurrence of an additional absorption profile within an EIT window. Boon *et al.*[28] reported a theoretical study on the effect of wavelength mismatch between the control field and the probe field on the probe transparency profile for the three basic level schemes Ξ, Λ, and Vee under a strong control field regime. EIT using Cs under Doppler free and Doppler broadened conditions was reported by Clarke *et al.*[29] for wavelength mismatched control and

*Project supported by UGC, New Delhi, India.
†Corresponding author. E-mail: mondal.suman27@gmail.com
‡Corresponding author. E-mail: arindam.ghosh.phy@gmail.com
§Corresponding author. E-mail: m2amitava@gmail.com
© 2018 Chinese Physical Society and IOP Publishing Ltd

probe fields. Effects of the very strong control field as well as its detuning on the probe absorption profile were shown in that article. Niu *et al.*[30] investigated the effect of Doppler broadening on Autler–Towns splitting[26] in six-wave mixing in a cascade four-level system as well as a folded four-level system. Three different resonant fields were applied to the systems concerned. Their dressed state model can be used to explain the strong wave number ratio dependence of the Autler–Towns splitting in the six-wave mixing spectrum. In this work, we show through analytic calculation how the wavelength mismatch between the probe and pump (control) beams can produce an enhanced absorption like feature instead of EIT at a control field Rabi frequency ten times higher than that of the probe field by using the transition parameters like spontaneous decay rates and relative transition strengths of ^{133}Cs, but under a similar situation it is shown that for the transitions of ^{87}Rb, one gets transparency. The role of different velocity groups of atoms towards probe absorption is also shown. The effect of extra ground level on the probe absorption in a Ξ type system is also presented. When the intensity of the probe field is made greater than the pump field, an enhanced absorption peak formed on the simulated Doppler averaging background is noticed for the $n^2S_{1/2} \rightarrow n^2P_{3/2} \rightarrow n^2D_{5/2}$ transitions of both ^{133}Cs and ^{87}Rb, where the principal quantum number $n = 5$ for ^{87}Rb and $n = 6$ for ^{133}Cs. This absorption peak widens and shows a dip at its middle when the probe field intensity is increased further.

2. Theoretical analysis

The interaction Hamiltonian for the three-level Ξ type system (shown in Fig. 1) can be written as follows:

$$H_{\mathrm{T}} = H_0 + H_1 + H_2. \tag{1}$$

Here H_0 is the Hamiltonian of the unperturbed system, whereas H_1 and H_2 represent the perturbations due to the interaction of the probe and control fields with the three-level atomic system, respectively,

$$H_0 = \hbar\omega_1|1\rangle\langle 1| + \hbar\omega_2|2\rangle\langle 2| + \hbar\omega_3|3\rangle\langle 3|, \tag{2}$$

$$H_1 = -\frac{\hbar}{2}\left[|2\rangle\langle 1|\Omega_1 \mathrm{e}^{-\mathrm{i}\omega_{\mathrm{p}}t} + \mathrm{c.c.}\right], \tag{3}$$

$$H_2 = -\frac{\hbar}{2}\left[|3\rangle\langle 2|\Omega_2 \mathrm{e}^{-\mathrm{i}\omega_{\mathrm{c}}t} + \mathrm{c.c.}\right]. \tag{4}$$

The energies of the three states $|1\rangle$, $|2\rangle$ and $|3\rangle$ are given by $\hbar\omega_1$, $\hbar\omega_2$, and $\hbar\omega_3$, respectively. The probe field has a Rabi frequency of Ω_1 and a circular frequency of ω_{p}, whereas the Rabi frequency of the control or pump field is represented by Ω_2 and its circular frequency is given by ω_{c}. Here the Rabi frequencies are defined by $\Omega_x = \mu_{ij}E_x/\hbar$, x stands for probe ($x = 1$) or control ($x = 2$) field, μ_{ij} is the transition dipole matrix element associated with the transition $|j\rangle \rightarrow |i\rangle$. E_x stands for the electric field amplitude for the probe ($x = \mathrm{p}$) or control ($x = \mathrm{c}$) field. The Rabi frequencies are taken to be real here. The probe frequency detuning under the Doppler free condition is given by $\Delta_1 = \omega_{\mathrm{p}} - \omega_{21}$, where $\omega_{21} = \omega_2 - \omega_1$.[7] The control frequency detuning under a similar condition is $\Delta_2 = \omega_{\mathrm{c}} - \omega_{32}$, where $\omega_{32} = \omega_3 - \omega_2$. The time evolution of the density matrix operator ρ of the system is governed by the Liouville equation (or the Master equation) with the phenomenological decay terms added

$$\frac{\partial\rho}{\partial t} = -\frac{\mathrm{i}}{\hbar}[H,\rho] + \Lambda_{\mathrm{relax}}\rho. \tag{5}$$

The term Λ_{relax} stands for the relaxation operator. A set of 9 optical Bloch equations (OBE) for the three-level Ξ system are derived by using Eqs. (1)–(5) and then solved analytically under steady state condition (i.e., $\partial\rho/\partial t = 0$) by using the condition of population conservation $\sum_{i=1}^{3}\rho_{ii} = 1$ in order to determine the probe response term ρ_{21}.[31]

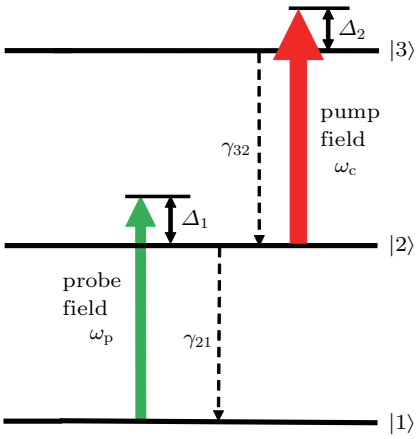


Fig. 1. (color online) Three-level Ξ type system.

The addition of an extra ground level to the three-level Ξ type system makes it look like that shown in Fig. 2. The only modification in the Hamiltonian of this system will be the addition of one term in the unperturbed Hamiltonian (Eq. (2)) as given below:

$$\begin{aligned} H_0 = {} & \hbar\omega_0|0\rangle\langle 0| + \hbar\omega_1|1\rangle\langle 1| \\ & + \hbar\omega_2|2\rangle\langle 2| + \hbar\omega_3|3\rangle\langle 3|. \end{aligned} \tag{6}$$

Here the two ground energy levels are represented by level $|1\rangle$ and level $|0\rangle$ (Fig. 2). $\hbar\omega_0$ is the energy of the additional ground state $|0\rangle$. A set of 16 optical Bloch equations can be derived for this four-level system starting from the Master equation (Eq. (5))

$$\begin{aligned} \frac{\partial\rho_{11}}{\partial t} = {} & -\gamma_{10}\rho_{11} + \gamma_{21}\rho_{22} + \gamma_{01}\rho_{00} \\ & + \frac{\mathrm{i}\Omega_1}{2}(\rho_{21} - \rho_{12}), \\ \frac{\partial\rho_{22}}{\partial t} = {} & -(\gamma_{21} + \gamma_{20})\rho_{22} + \gamma_{32}\rho_{33} \end{aligned} \tag{7}$$

$$+\frac{\mathrm{i}\Omega_1}{2}(\rho_{12}-\rho_{21})-\frac{\mathrm{i}\Omega_2}{2}(\rho_{23}-\rho_{32}), \quad (8)$$

$$\frac{\partial\rho_{33}}{\partial t} = -\gamma_{32}\rho_{33}+\frac{\mathrm{i}\Omega_2}{2}(\rho_{23}-\rho_{32}), \quad (9)$$

$$\frac{\partial\rho_{00}}{\partial t} = \gamma_{10}\rho_{11}+\gamma_{20}\rho_{22}-\gamma_{01}\rho_{00}, \quad (10)$$

$$\frac{\partial\rho_{21}}{\partial t} = \mathrm{i}\left[\Delta_1+\frac{\mathrm{i}(\gamma_{21}+\gamma_{20}+\gamma_{10})}{2}\right]\rho_{21} +\mathrm{i}\frac{\Omega_2}{2}\rho_{31}+\mathrm{i}\frac{\Omega_1}{2}(\rho_{11}-\rho_{22}), \quad (11)$$

$$\frac{\partial\rho_{31}}{\partial t} = \mathrm{i}\left[(\Delta_1+\Delta_2)+\frac{\mathrm{i}(\gamma_{32}+\gamma_{10})}{2}\right]\rho_{31} +\mathrm{i}\frac{\Omega_2}{2}\rho_{21}-\mathrm{i}\frac{\Omega_1}{2}\rho_{32}, \quad (12)$$

$$\frac{\partial\rho_{32}}{\partial t} = \mathrm{i}\left[\Delta_2+\frac{\mathrm{i}(\gamma_{21}+\gamma_{20}+\gamma_{32})}{2}\right]\rho_{32} -\mathrm{i}\frac{\Omega_1}{2}\rho_{31}-\mathrm{i}\frac{\Omega_2}{2}(\rho_{33}-\rho_{22}), \quad (13)$$

$$\frac{\partial\rho_{01}}{\partial t} = \mathrm{i}\left[\Delta_1+\frac{\mathrm{i}(\gamma_{01}+\gamma_{10})}{2}\right]\rho_{01}-\mathrm{i}\frac{\Omega_1}{2}\rho_{02}, \quad (14)$$

$$\frac{\partial\rho_{20}}{\partial t} = \mathrm{i}\frac{\Omega_1}{2}\rho_{10}+\mathrm{i}\frac{\Omega_2}{2}\rho_{30}-\frac{(\gamma_{21}+\gamma_{20}+\gamma_{01})}{2}\rho_{20}, \quad (15)$$

$$\frac{\partial\rho_{30}}{\partial t} = \mathrm{i}\left[\Delta_2+\frac{\mathrm{i}(\gamma_{01}+\gamma_{32})}{2}\right]\rho_{30}+\mathrm{i}\frac{\Omega_2}{2}\rho_{20}. \quad (16)$$

Equations (11)–(16) have their transpose conjugates too, which are not shown here. To determine the probe response term ρ_{21}, these equations are solved under the steady state condition (i.e., $\partial\rho/\partial t = 0$) by using an analytical technique, subject to the condition of population conservation $\sum_{i=0}^{3}\rho_{ii}=1$. The imaginary and real parts of ρ_{21} are responsible for the absorption (α) and dispersion (β) of the probe field,

$$\alpha = \frac{4\pi\omega_\mathrm{p}}{c}\,\mathrm{Im}(\rho_{21}), \quad (17)$$

$$\beta = \frac{4\pi\omega_\mathrm{p}}{c}\,\mathrm{Re}(\rho_{21}). \quad (18)$$

Equation (17) can be used to determine the probe absorption under the Doppler free condition. If the atoms are kept in a vapor cell at absolute temperature T, the thermal motion of the atoms would cause Doppler averaging. Assume that the atoms follow the Maxwell distribution, the Doppler averaging can be included into the calculation in the following manner:

$$\alpha_\mathrm{d} = \int_{-\infty}^{\infty}\alpha M(v)\,\mathrm{d}v, \quad (19)$$

$$\beta_\mathrm{d} = \int_{-\infty}^{\infty}\beta M(v)\,\mathrm{d}v, \quad (20)$$

where α_d and β_d stand for the probe absorption and probe dispersion under Doppler averaging. Here $M(v) = \left(u\sqrt{\pi}\right)^{-1}\mathrm{e}^{-v^2/u^2}$. The u is the most probable velocity of the atoms at temperature T, $u=\sqrt{2RT/M}$, where R is the universal gas constant and M is the molar mass of the atomic gas. v stands for the velocity of any atom. The value of v can ideally be anything starting from $-\infty$ to $+\infty$. In this work, we are mainly interested in probe absorption under different conditions. The imaginary part of ρ_{21} is given as

$$\mathrm{Im}(\rho_{21}) = \frac{\left[\frac{\Omega_1\Omega_2^2}{4}\frac{\gamma_2}{(\Delta_1+\Delta_2)^2+\gamma_2^2}+\gamma_1\Omega_1\right](\rho_{11}-\rho_{22})}{2\left[(\Delta_1^2+\gamma_1^2)+\frac{\Omega_2^4}{16}\frac{1}{\left\{(\Delta_1+\Delta_2)^2+\gamma_2^2\right\}}-\frac{\Omega_2^2}{2}\frac{\{(\Delta_1+\Delta_2)\Delta_1-\gamma_1\gamma_2\}}{\left\{(\Delta_1+\Delta_2)^2+\gamma_2^2\right\}}\right]}. \quad (21)$$

By using this expression in Eq. (17), we can simulate probe absorption under the Doppler free condition. Equation (17) can be used to put the expression for α in Eq. (19) to find out the probe absorption at temperature T. Here Δ_1 and Δ_2 are the detunings of the probe and control fields respectively but the corresponding Doppler shifts are given by $\mp vk_\mathrm{p}$ and $\pm vk_\mathrm{c}$. k_p and k_c are the propagation constants of the probe and the control fields, respectively. Thus while taking the Doppler broadening into account, the detunings of the probe and control fields must be taken as $\Delta_1=\omega_\mathrm{p}-\omega_{21}\mp vk_\mathrm{p}$ and $\Delta_2=\omega_\mathrm{c}-\omega_{32}\pm vk_\mathrm{c}$.[7,25] $\gamma_1=\frac{\gamma_{21}+\gamma_{20}+\gamma_{10}}{2}$, $\gamma_2=\frac{\gamma_{32}+\gamma_{10}}{2}$, where γ_{21} and γ_{20} stand for the spontaneous decay rates to the two ground levels $|1\rangle$ and $|0\rangle$ from the intermediate level $|2\rangle$ (Fig. 2). The spontaneous decay rate from the uppermost level $|3\rangle$ to the intermediate level $|2\rangle$ is γ_{32} (Fig. 2). γ_{10} and γ_{01} represent the non-radiative decay rates between the two ground states $|1\rangle$ and $|0\rangle$ respectively.

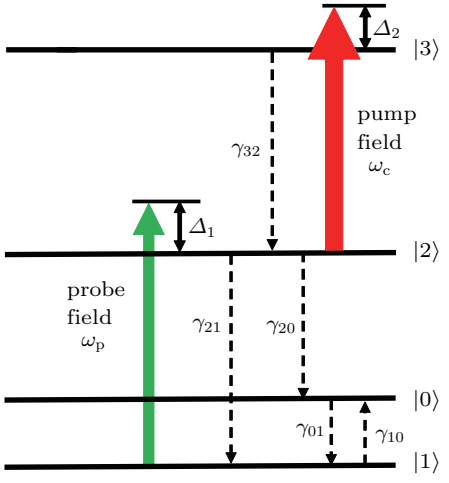


Fig. 2. (color online) Four-level Ξ type system.

3. Results

We have used the line parameters of three Ξ type transitions to study the probe absorption for a simple three-level Ξ type system and the effect of an extra ground level (thereby transforming the three-level system into a four-level system) on the probe absorption. The three transitions are (A) ^{133}Cs $6^2S_{1/2} \rightarrow 6^2P_{3/2} \rightarrow 6^2D_{5/2}$, (B) ^{87}Rb $5^2S_{1/2} \rightarrow 5^2P_{3/2} \rightarrow 7^2S_{1/2}$, and (C) ^{87}Rb $5^2S_{1/2} \rightarrow 5^2P_{3/2} \rightarrow 5^2D_{5/2}$. Here we just want to mention that these three level schemes are actually multi-level systems each having two ground levels. The wavelength for the $6^2S_{1/2} \rightarrow 6^2P_{3/2}$ transition for ^{133}Cs is 852 nm,[32] whereas that for the $6^2P_{3/2} \rightarrow 6^2D_{5/2}$ transition is 917 nm (case-A). For ^{87}Rb, the wavelength for the $5^2S_{1/2} \rightarrow 5^2P_{3/2}$ transition is 780 nm[33] and that for the $5^2P_{3/2} \rightarrow 5^2D_{5/2}$ is 776 nm[34] (case-C). The $5^2P_{3/2} \rightarrow 7^2S_{1/2}$ transition of ^{87}Rb occurs at 741 nm[34] (case-B). Hence, the propagation constants k_p and k_c of the probe and control fields differ from each other and their difference is substantial for the first two cases (case-A and case-B) compared to that of case-C. For the four-level Ξ type system, we have taken the values of γ_{21} and γ_{20} for ^{133}Cs from Ref. [32] and those for ^{87}Rb from Ref. [33]. The value of γ_{32} for ^{133}Cs is taken from Ref. [35]. For ^{87}Rb, γ_{32} would assume two different values for the two different spontaneous transitions $5^2D_{5/2} \rightarrow 5^2P_{3/2}$[36] and $7^2S_{1/2} \rightarrow 5^2P_{3/2}$.[37] We have not allowed spontaneous decay of population from the uppermost level $|3\rangle$ to the ground levels ($|1\rangle$ and $|0\rangle$) because of the dipole selection rule. The values of γ_{10} and γ_{01} are kept fixed at 0.01 MHz throughout the simulation if not specified separately. Furthermore, we have kept the probe Rabi frequency (Ω_1) fixed at 1 MHz if not mentioned otherwise. The probe and control fields are taken to be counter-propagating.

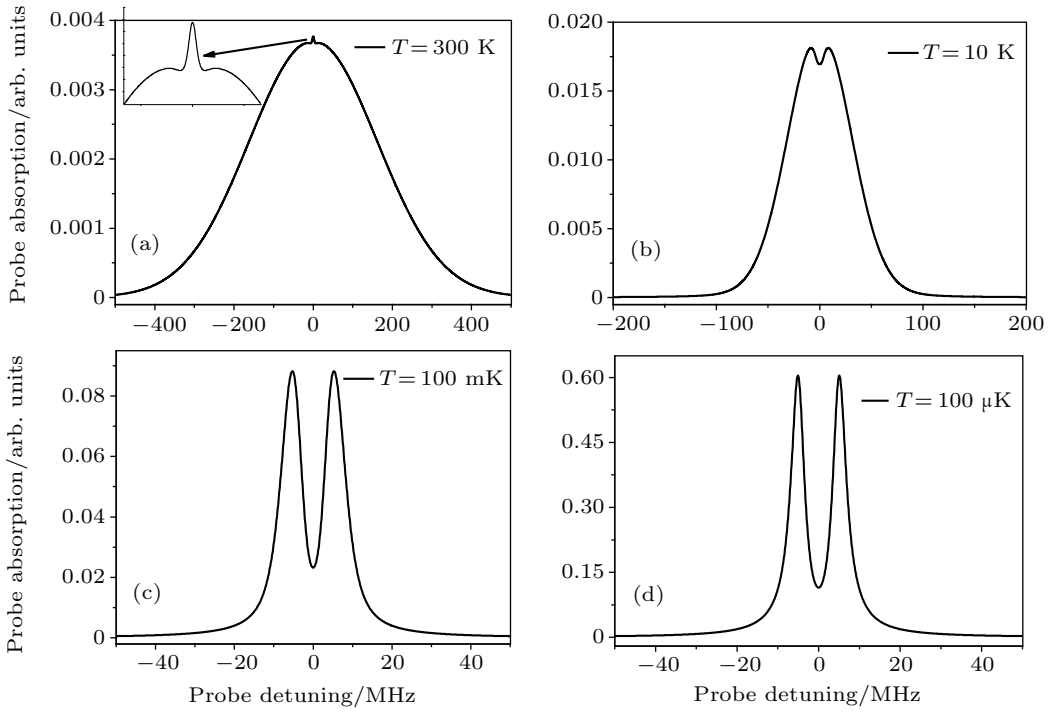


Fig. 3. Probe absorption of three-level Ξ type system at four different temperatures: (a) $T = 300$ K, (b) $T = 10$ K, (c) $T = 100$ mK, and (d) $T = 100$ μK for ^{133}Cs. $\Omega_1 = 1$ MHz and $\Omega_2 = 10$ MHz.

Figure 3 shows the probe absorption for ^{133}Cs at four different temperatures using the three-level Ξ type system at a control Rabi frequency (Ω_2) of 10 MHz. Here the most striking part is the formation of an enhanced absorption like peak at the zero probe detuning ($\Delta_1 = 0$ MHz) at $T = 300$ K. This enhanced absorption converts into an EIT at lower temperature under the two-photon resonance condition. The formation of EIT under two-photon resonance is quite obvious,[1] but its transformation into an enhanced absorption like feature near room temperature is due to the residual Doppler averaging which becomes prominent at higher temperature. Plots of probe absorption at $T > 300$ K obviously show this enhanced absorption like feature at two-photon resonance (not shown here). Enhancement in probe absorption from a transparency background for ^{85}Rb under the strong-probe condition was reported by Pandey *et al.*[21] in a room temperature vapor cell but we are observing this feature for ^{133}Cs under the weak probe condition. There are reports on probe absorption in cold Rb vapor showing multiple EIT,[38] but no enhanced absorption was found. For ^{87}Rb, the simulation shows the usual EIT for the $5^2S_{1/2} \rightarrow 5^2P_{3/2} \rightarrow 5^2D_{5/2}$ transition but when the parameters, specifically, the wavelengths of the $5^2S_{1/2} \rightarrow 5^2P_{3/2} \rightarrow 7^2S_{1/2}$ transitions are used in the simulation, the EIT window appears under the background of enhanced absorption at $T = 300$ K with $\Omega_1 = 1$ MHz and $\Omega_2 = 10$ MHz (Fig. 4). Thus the change in specimen and

transition parameters drastically modifies the probe absorption feature. The longer lifetime of the uppermost energy level $|3\rangle$ of ^{87}Rb makes the coherence dephasing rate of the dipole forbidden transition[1,39] between $|3\rangle$ and $|1\rangle$ be smaller than that of ^{133}Cs, thereby making ^{87}Rb more favorable for the observation of EIT in the three-level Ξ type system. That is why even at $\Omega_1 = 1$ MHz and $\Omega_2 = 10$ MHz EIT is observed in the simulated probe absorption for ^{87}Rb (Fig. 4), whereas ^{133}Cs does not show any transparency (Fig. 3(a)).

It is to be remembered that for the two different transitions of ^{87}Rb, the wavelength of the control field (acting from $|2\rangle$ to $|3\rangle$, Fig. 1) is smaller than that of the probe beam (acting from $|1\rangle$ to $|2\rangle$, Fig. 1), whereas for ^{133}Cs, the reverse is true, i.e., the wavelength of the probe field is smaller than that of the control field. In Fig. 5, the contribution towards probe absorption by different velocity groups of atoms in the case of ^{133}Cs and ^{87}Rb is shown at $T = 300$ K. From this figure, we can see how the contribution towards enhanced probe absorption for ^{133}Cs turns into a transparency in the case of ^{87}Rb around $\Delta_1 = 0$. The effect of residual Doppler averaging on the absorption line shape for the $5^2S_{1/2} \rightarrow 5^2P_{3/2} \rightarrow 7^2S_{1/2}$ transition is more significant than that of the $5^2S_{1/2} \rightarrow 5^2P_{3/2} \rightarrow 5^2D_{5/2}$ transition because of greater wavelength mismatch between the control and probe beams for the former. This is quite evident in the absorption line shapes around $\Delta_1 = 0$ where a strong EIT signal is formed in the background of an enhanced absorption peak for the former (olive curve in Fig. 4) but much weaker EIT is seen for the latter with no enhanced absorption like feature (red curve in Fig. 4) like the former.

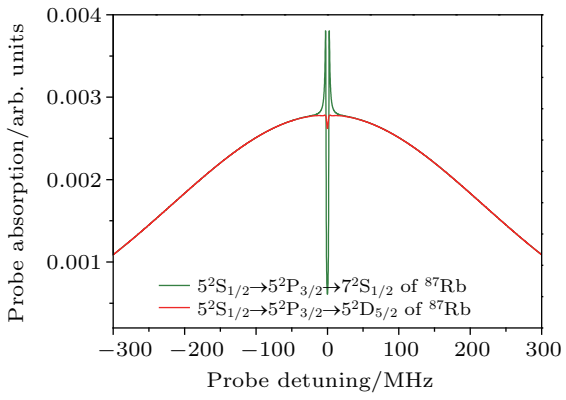


Fig. 4. (color online) Probe absorption of the three-level Ξ type system at $T = 300$ K for two different transitions (case-B and case-C) as mentioned in the figure. $\Omega_1 = 1$ MHz and $\Omega_2 = 10$ MHz.

From Fig. 5, it is seen that the effects of different velocity groups of atoms are different for the three different transitions, case-A: ^{133}Cs $6^2S_{1/2} \rightarrow 6^2P_{3/2} \rightarrow 6^2D_{5/2}$ (control wavelength 917 nm, probe wavelength 852 nm), case-B: ^{87}Rb $5^2S_{1/2} \rightarrow 5^2P_{3/2} \rightarrow 7^2S_{1/2}$ (control wavelength 741 nm, probe wavelength 780 nm), case-C: ^{87}Rb $5^2S_{1/2} \rightarrow 5^2P_{3/2} \rightarrow 5^2D_{5/2}$ (control wavelength 776 nm, probe wavelength 780 nm) at $\Omega_1 = 1$ MHz and $\Omega_2 = 10$ MHz for each case. With the help of these graphs, it is easier to understand how the effect of velocity is altering the probe absorption in the three different cases as mentioned in Figs. 5(a)–5(c). When the contribution of the $v = +10$ m/s group of atoms towards probe absorption is plotted along with the $v = 0$ m/s velocity groups of atoms (Fig. 5(d)) for the three different transitions just mentioned, we can easily see the reason why we obtain an enhanced absorption like peak around zero probe detuning ($\Delta_1 = 0$) in case-A instead of the EIT like feature and indeed we find EIT for case-C. For case-B, however, the contributions of velocity groups differ from the corresponding velocity groups of case-C and the cumulative effect of this difference over the entire velocity spectrum substantially modifies the EIT window as compared to case-C. The effect of wavelength mismatch between the control and probe laser fields has also been shown by Urvoy *et al.*[40] using an open three-level Ξ type system. In multi-level systems, the spectra get altered accordingly.[41]

The situation is modified significantly in case-A if an additional ground level is added to the simple three-level Ξ type system. It is to be remembered that the alkali ground state is an $S_{1/2}$ state, which has two hyperfine levels. So, for alkali atoms, for all practical purposes, we shall have to consider two ground hyperfine levels in analyzing a Ξ type system. For case-A, the transition wavelength from the middle state ($|2\rangle$ in Fig. 2) to the uppermost state ($|3\rangle$ in Fig. 2) is greater than the transition wavelength from one of the ground states ($|1\rangle$ in Fig. 2) to the middle state ($|2\rangle$ in Fig. 2). For this case, the enhanced absorption is no more seen in the simulated probe absorption curve (compare Fig. 6(a) with Fig. 3(a)) at $\Omega_1 = 1$ MHz and $\Omega_2 = 10$ MHz. In fact, no EIT is found either (black curve in Fig. 6(a)). With the increase in the control Rabi frequency, the probe absorption starts showing transparency, which gets stronger as the control Rabi frequency is increased further (Fig.6(a)). This transparency is due to the creation of usual Autler–Towns doublets[26] at higher control field intensity. However, for a different specimen like ^{87}Rb with the $5^2S_{1/2} \rightarrow 5^2P_{3/2} \rightarrow 5^2D_{5/2}$ transition (case-C) parameters used in the simulation (control wavelength (776 nm) is less but very near to the wavelength of the probe field (780 nm)), we get a transparency signal in the probe absorption curve even at $\Omega_1 = 1$ MHz, $\Omega_2 = 10$ MHz and this transparency line shape resembles the conventional EIT signal at comparatively higher control Rabi frequency too. The interesting point is that if we interchange the wavelengths of the probe and control fields in Fig. 6(a), the feature of the probe absorption curve becomes more like that of the green curve in Fig. 4. This undoubtedly establishes the influence of wavelength mismatch in the absorption line profile.

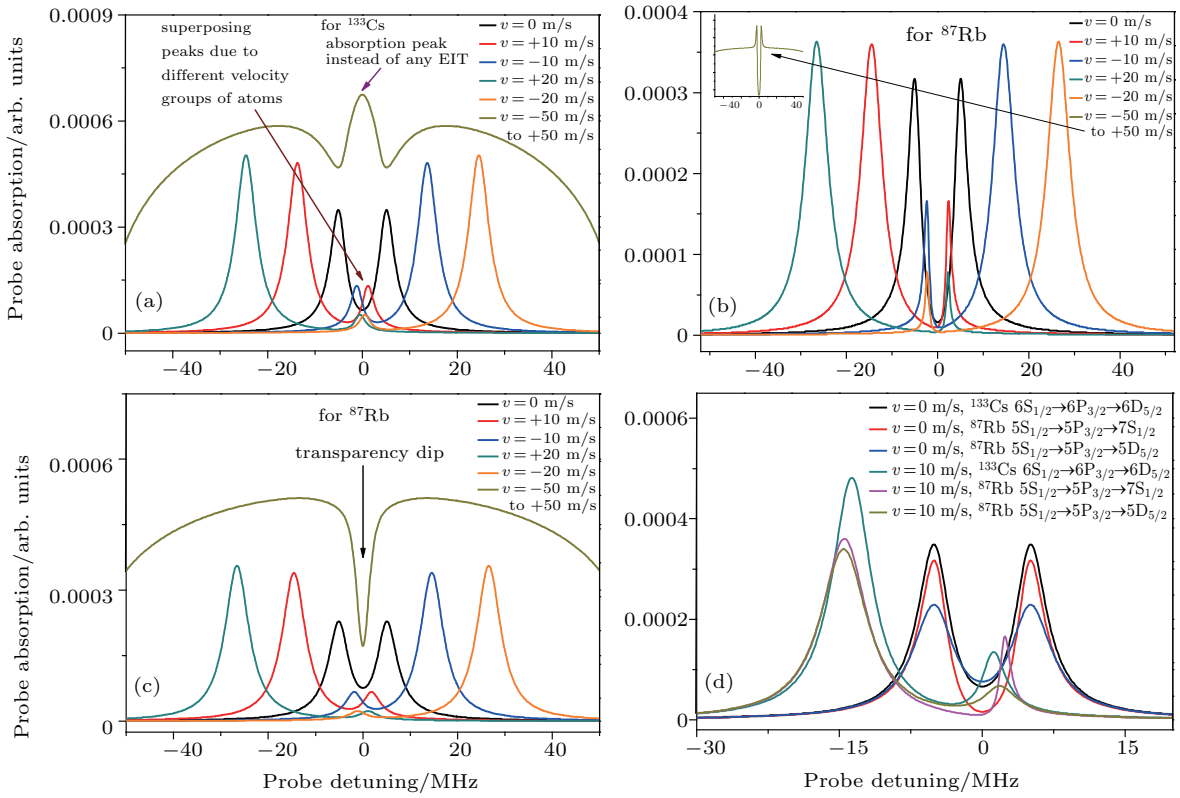


Fig. 5. (color online) Effect of velocity for the three-level Ξ type system in (a) ^{133}Cs $6^2S_{1/2} \rightarrow 6^2P_{3/2} \rightarrow 6^2D_{5/2}$, (b) ^{87}Rb $5^2S_{1/2} \rightarrow 5^2P_{3/2} \rightarrow 7^2S_{1/2}$, (c) ^{87}Rb $5^2S_{1/2} \rightarrow 5^2P_{3/2} \rightarrow 5^2D_{5/2}$. (d) Difference in absorption due to two different velocity groups of atoms: $v = 0$ m/s and $v = +10$ m/s for the three different cases as mentioned in the figure. $\Omega_1 = 1$ MHz and $\Omega_2 = 10$ MHz.

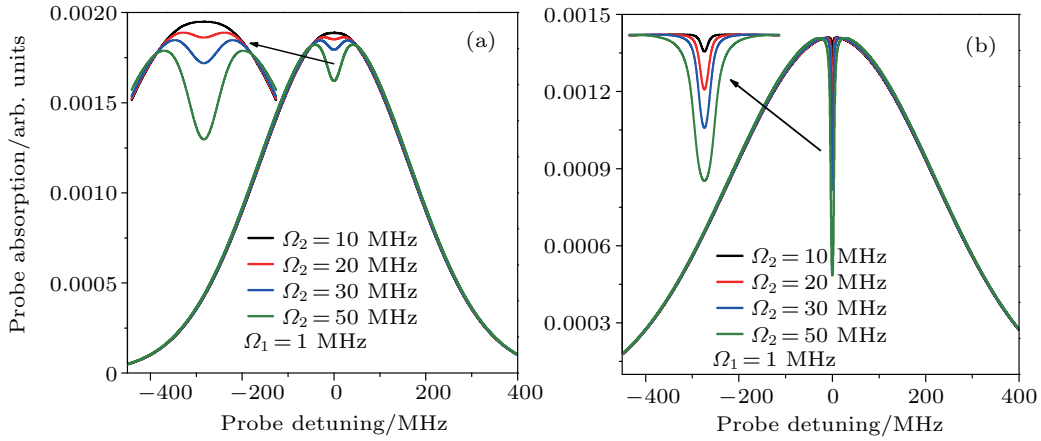


Fig. 6. (color online) Probe absorption at different control Rabi frequencies for four-level Ξ type system at $T = 300$ K for (a) ^{133}Cs $6^2S_{1/2} \rightarrow 6^2P_{3/2} \rightarrow 6^2D_{5/2}$ and (b) ^{87}Rb $5^2S_{1/2} \rightarrow 5^2P_{3/2} \rightarrow 5^2D_{5/2}$. $\Omega_1 = 1$ MHz.

If now the roles of the control and probe fields are reversed, i.e., Ω_1 is made greater than Ω_2, we can get some features in the probe absorption for the three-level Ξ type system which are not obtained for the usual case of $\Omega_1 \ll \Omega_2$. We begin with case-A: ^{133}Cs $6^2S_{1/2} \rightarrow 6^2P_{3/2} \rightarrow 6^2D_{5/2}$. In Fig. 7, plots of probe absorption vs. probe detuning under the Doppler free condition as well as under the Doppler averaging are shown. Under the Doppler free condition, we get probe absorption curves resembling a Lorentzian line profile, no transparency appears. Obviously, in absence of the control field ($\Omega_2 = 0$), the probe absorption is enhanced. This enhancement is prominent when the difference between the control and probe Rabi frequencies is less. However, under Doppler averaging (at $T = 300$ K), the simulated probe absorption curves show distinctly different features, there is a hint of transparency near zero probe detuning from which the probe absorption suddenly rises, but around $\Delta_1 = 0$ probe absorption dips (Fig. 7(c)) again. If the probe Rabi frequency is increased (Fig. 7(d)), not only the width of the transparency like window increases but the central dip in absorption also widens. This may have a useful application in manipulating the probe pulse propagation in a Doppler broadened alkali vapor medium.

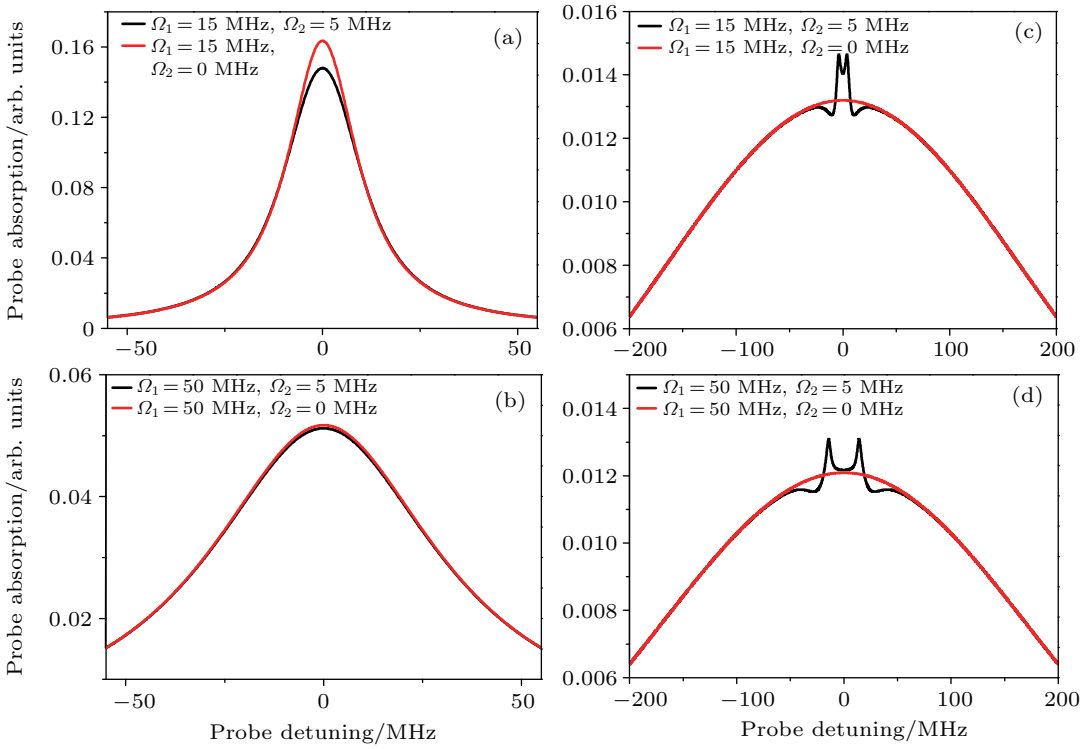


Fig. 7. (color online) Probe absorption vs. probe detuning for ^{133}Cs $6^2S_{1/2} \rightarrow 6^2P_{3/2} \rightarrow 6^2D_{5/2}$ transitions under (a), (b) Doppler free and (c), (d) Doppler averaged conditions for the three-level Ξ type system.

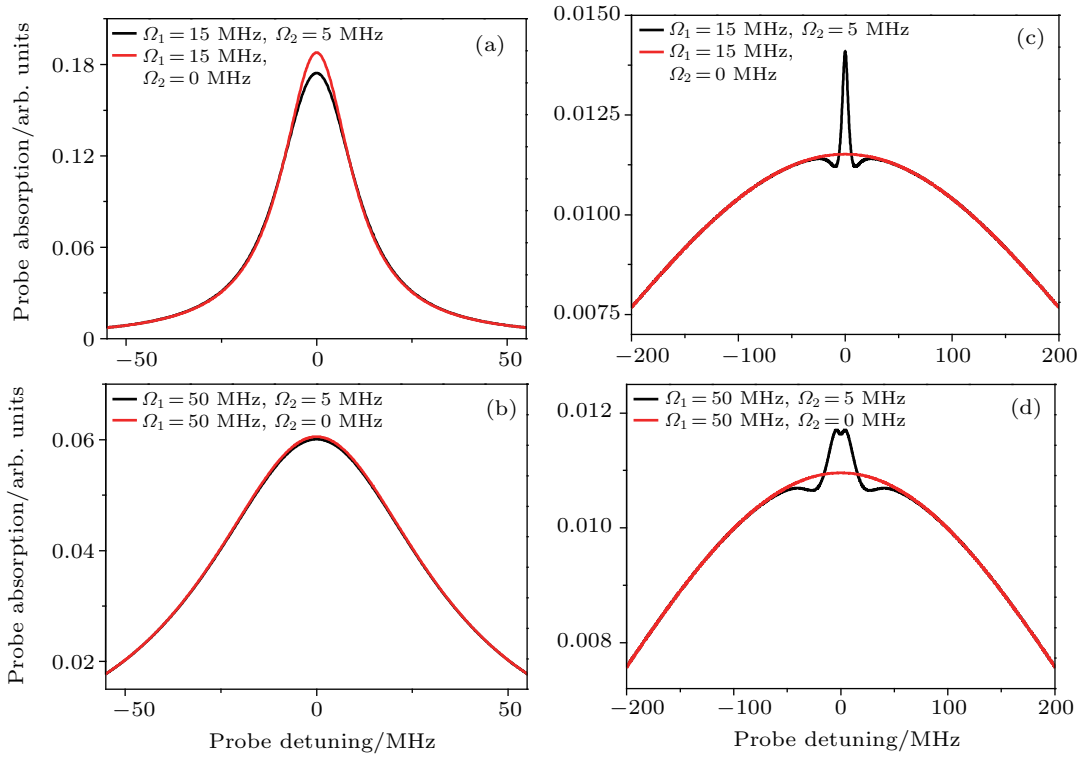


Fig. 8. (color online) Probe absorption vs. probe detuning for ^{87}Rb $5^2S_{1/2} \rightarrow 5^2P_{3/2} \rightarrow 5^2D_{5/2}$ transitions under (a), (b) Doppler free and (c), (d) Doppler averaged conditions for the three-level Ξ type system.

The effect of residual Doppler averaging resulting from wavelength mismatch causes a distinctly different feature in the simulated absorption line shape of the probe field for the three-level Ξ type system when we use the parameters of ^{87}Rb $5^2S_{1/2} \rightarrow 5^2P_{3/2} \rightarrow 5^2D_{5/2}$ transitions (case-C) in the simulation (Fig. 8). This shows the crucial role played by this mechanism in absorption spectroscopy. Simulated probe absorptions under the Doppler free condition for these transitions of ^{87}Rb at $\Omega_2 = 5$ MHz, $\Omega_1 = 15$ MHz and $\Omega_2 = 5$ MHz, $\Omega_1 = 50$ MHz are given in Figs. 8(a) and 8(b), respectively.

Comparing Fig. 8(c) with Fig. 7(c), it is observed that the probe absorption suddenly rises from a transparency like background near zero probe detuning under the Doppler broadened condition but unlike Fig. 7(c) there is no central dip in the absorption peak for $\Omega_2 = 5$ MHz and $\Omega_1 = 15$ MHz. With the increase in the value of Ω_1 (Fig. 8(d)), the central enhanced absorption gets wider and a small dip at $\Delta_1 = 0$ occurs. However, this small dip in probe absorption is indeed much smaller than the central absorption dip at $\Delta_1 = 0$ in Fig. 7(d). We can investigate this more deeply if we compare the contribution towards probe absorption around zero probe detuning by the different velocity groups of atoms for the two cases.

For the four-level Ξ type system, however there is marked difference in the simulated probe absorption line shape under the high probe field regime (Fig. 9) as compared to the three-level system (Fig. 8). Under the Doppler free condition, the probe absorption shows a transparency window (Fig. 9(a)) at $\Omega_2 = 5$ MHz and $\Omega_1 = 15$ MHz. The transparency window widens and its depth increases at $\Omega_2 = 15$ MHz and $\Omega_1 = 50$ MHz (Fig. 9(b)). Under Doppler averaging, the simulated probe absorption shows the signature of transparency, which increases at $\Omega_2 = 15$ MHz and $\Omega_1 = 50$ MHz. The transparency window resembles the EIT line shape.

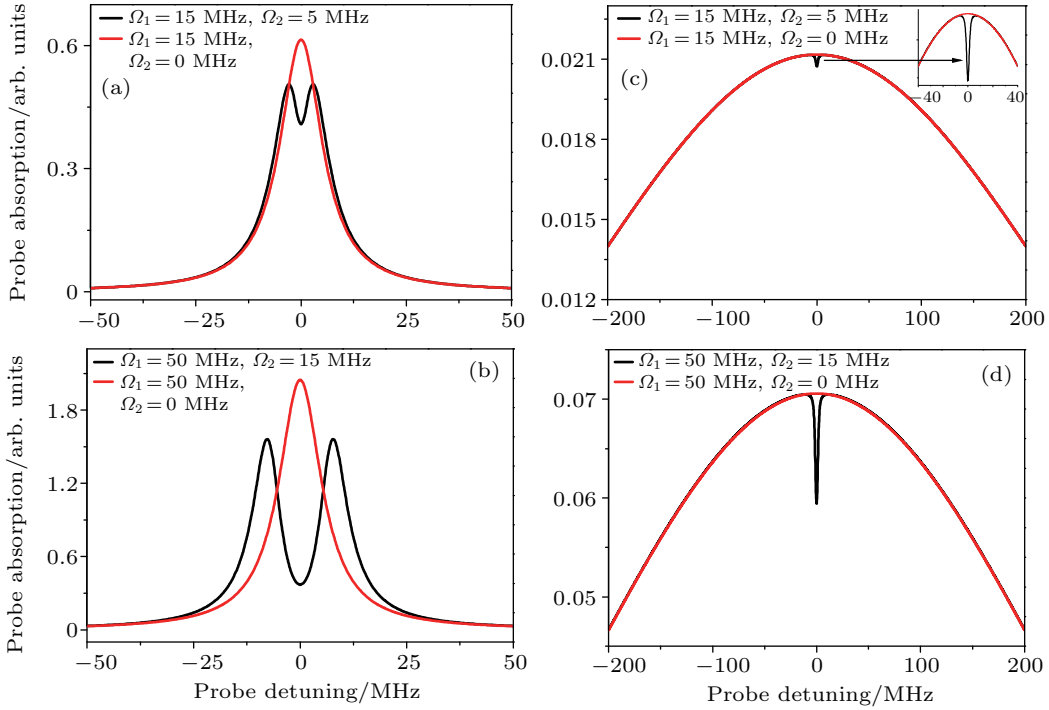


Fig. 9. (color online) Probe absorption vs. probe detuning for ^{87}Rb $5^2S_{1/2} \rightarrow 5^2P_{3/2} \rightarrow 5^2D_{5/2}$ transitions under (a), (b) Doppler free and (c), (d) Doppler averaged conditions for the four-level Ξ type system.

The addition of the extra ground level in a three-level Ξ type system largely redistributes the population in the ground levels in the presence of the control and probe fields. In fact, optical pumping starts building up the population in the other ground level (level $|0\rangle$ in Fig. 2) and it reaches a maxima around zero probe detuning ($\Delta_1 = 0$). With other conditions remaining the same, this leads to a loss of population from the other ground level ((level $|1\rangle$ in Fig. 2) as well as from the emission-absorption cycle of the laser fields. This causes a dip in the probe absorption in the four-level Ξ type system.

4. Conclusion

In summary, we have shown the effect of wavelength mismatch between two coherent fields forming a simple three-level Ξ type system using three different sets of transition parameters out of which two cases are just opposite to each other, i.e., in one case the upper laser wavelength is considerably greater than the wavelength of the laser that is acting from the ground level and vice versa for the other case. For the third case, the wavelength of the laser that is acting from the ground level is slightly greater than the other. The effects of residual Doppler averaging under wavelength mismatch in three different sets of transitions show distinctly different absorption line shapes. With the addition of the extra ground level, the simulated probe absorption under the Doppler broadened condition shows a transparency window for both ^{133}Cs and ^{87}Rb, but one does not resembles the other transparency line shape for the same control and probe intensities. Thus the choice of sample as well as the choice of transition wavelength both affect the probe absorption in a Ξ type system. The most interesting part is the enhanced absorption peak bulging out from the middle of the Doppler averaged probe absorption profile

for ^{133}Cs for three-level Ξ type system at $\Omega_2 = 10$ MHz and $\Omega_1 = 1$ MHz, a feature which has not been reported earlier and we have referred to it as enhanced probe absorption. However, at higher control field intensity it quickly disappears and the transparency appears. The four-level Ξ type system shows a transparency window under both Doppler free and Doppler averaging conditions in the high probe field regime, making it considerably different from the three-level system. The models discussed here can be used to compare the experimental findings. More studies on such systems are expected in the future.

Acknowledgment

SM thanks the University Grants Commission, New Delhi for providing the research fellowship (JRF-NET, vide sanction No. F. 17-124/2008(SA-I) dated 22/08/2014). AB acknowledges the University Grants Commission, New Delhi for awarding a major research project (F. No. -43-527/2014(SR) dated 28/09/2015).

References

[1] Fulton D J, Shepherd S, Moseley R R, Sinclair B D and Dunn M H 1995 *Phys. Rev. A* **52** 2302
[2] Natarajan V 2015 *Modern Atomic Physics* (New York: CRC Press)
[3] Scully M O and Zubairy S 1997 *Quantum Optics* (Cambridge: Cambridge University Press)
[4] Imamoglu A and Harris S E 1989 *Opt. Lett.* **14** 1344
[5] Boller K J, Imamoglu A and Harris S E 1991 *Phys. Rev. Lett.* **66** 2593
[6] Agarwal G S and Harshawardhan 1996 *Phys. Rev. A* **77** 1039
[7] Bharati V and Wasan A 2014 *Opt. Commun.* **324** 238
[8] Joshi A and Xiao M 2003 *Phys. Lett. A* **317** 370
[9] Liu J B, Liu N, Shan C J, Huang Y X and Liu T K 2009 *J. Mod. Opt.* **56** 1774
[10] Ghosh A, Islam K, Bhattacharyya D and Bandyopadhyay A 2016 *J. Phys. B: At. Mol. Opt. Phys.* **49** 195401
[11] Hong Y, Dong Y, Mey Z, Bo F, Yan Z and Jin W 2012 *Chin. Phys. B* **21** 114207
[12] Li L, Guo H, Xiao F, Peng X and Chen X 2005 *J. Opt. Soc. Am. B* **22** 1309
[13] Chen Y, Wei X G and Ham B S 2009 *J. Phys. B: At. Mol. Opt. Phys.* **42** 065506
[14] Islam K, Bhattacharyya D, Ghosh A, Biswas D and Bandyopadhyay A 2017 *J. Phys. B: At. Mol. Opt. Phys.* **50** 215401
[15] Kash M M, Sautenkov V A, Zibrov A S, Hollberg L, Welch G R, Lukin M D, Rostovtsev Y, Fry E S and Scully O M 1999 *Phys. Rev. Lett.* **82** 5229
[16] Phillips D F, Fleischhauer A, Mair A and Walsworth R L 2001 *Phys. Rev. Lett.* **86** 783
[17] Novikova I, Walsworth R L and Xiao Y 2012 *Laser Photon. Rev.* **6** 333
[18] Harris S E, Field J E and Imamoglu A 1990 *Phys. Rev. Lett.* **64** 1107
[19] Zhang Y, Anderson B and Xiao M 2008 *Phys. Rev. A* **77** 061801
[20] Bhattacharyya D, Ghosh A, Bandyopadhyay A, Saha S and De S 2015 *J. Phys. B: At. Mol. Opt. Phys.* **48** 175503
[21] Pandey K and Natarajan V 2008 J. *Phys. B: At. Mol. Opt. Phys.* **41** 185504
[22] Salomaa R and Stenholm S 1976 *J. Phys. B: At. Mol. Phys.* **9** 1221
[23] Iftiquar S M, Karve G R and Natarajan V 2008 *Phys. Rev. A* **77** 063807
[24] Pack M V, Camacho R M and Howell J C 2007 *Phys. Rev. A* **76** 013801
[25] Shepherd S, Fulton D J and Dunn M H 1996 *Phys. Rev. A* **54** 5394
[26] Autler S H and Towns C H 1955 *Phys. Rev.* **100** 703
[27] Sandhya S N and Sharma K K 1997 *Phys. Rev. A* **55** 2155
[28] Boon J R, Zekou E, McGloin D and Dunn M H 1999 *Phys. Rev. A* **59** 4675
[29] Clarke J C and van Wijngaarden W A 2001 *Phys. Rev. A* **64** 023818
[30] Niu J, Pei L, Lu X, Wang R, Wu L A and Fu P 2011 *Phys. Rev. A* **84** 033853
[31] Ghosh A, Mondal S, Islam K, Mal K, Bhattacharyya D and Bandyopadhyay A 2016 *J. At. Mol. Conden. Nano Phys.* **3** 97
[32] Steck D A 2003 *Cesium D line data*
[33] Steck D A 2003 *Rubidium 87 D line data*
[34] Sansonetti J E and Martin W C 2005 *J. Phys. Chem. Ref. Data* **34** 1559
[35] Georgiades N Ph, Polzik E S and Kimble H J 1994 *Opt. Lett.* **19** 1474
[36] Sheng D, Perez Galvan A and Orozco L A 2008 *Phys. Rev. A* **78** 062506
[37] Safronova M S and Safronova U I 2011 *Phys. Rev. A* **83** 052508
[38] Wang J, Kong L B, Tu X H, Jiang K J, Li K, Xiong H W, Zhu Y and Zhan M S 2004 *Phys. Lett. A* **328** 437
[39] Yadav K and Wasan A 2017 *Phys. Lett. A* **381** 3246
[40] Urvoy A, Carr C, Ritter R, Adams C S, Weatherill K J and Low R 2013 *J. Phys. B: At. Mol. Opt. Phys.* **46** 245001
[41] Wang L R, Zhang Y C, Xiang S S, Cao S K, Xiao L T and Jia S T 2015 *Chin. Phys. B* **24** 063201